Plasma as a high-charge-state projectile stripping medium

G. D. Alton
Oak Ridge National Laboratory, Oak Ridge, Tennessee 37831-6368

R. A. Sparrow and R. E. Olson
University of Missouri, Rolla, Missouri 65401-0249

(Received 21 November 1991)

The classical trajectory Monte Carlo model has been used to computationally study the charge-state distributions that result from interactions between a high-energy, multielectron projectile and neutral and fully ionized targets. These studies are designed to determine the properties of a plasma for producing highly stripped ions as a possible alternative to gas and foil strippers that are commonly used to enhance the charge states of energetic ion beams. The results of these studies clearly show that a low-atomic-number, highly ionized plasma can yield higher charge states than a neutral target of the same density. The effect is principally attributable to the reduction in the number of available electron-capture channels. In this article, we compare the charge-state distributions that result during passage of a 20-MeV Pb projectile through neutral gas and fully ionized (singly charged) plasma strippers and estimate the effects of multiple scattering on the quality of the beam.

PACS number(s): 41.75.Ak, 52.40.Mj, 52.20.Hv, 34.50.Fa

I. INTRODUCTION

Since the final energy of an ion is related to the charge state of the ion during acceleration, the technique of employing a stripping medium (either solid or gaseous) between acceleration stages in heavy ion accelerators is frequently used. As an example, the final energy E_f of initially negatively charged atomic ions injected into a tandem electrostatic accelerator and stripped to charge state q in a single terminal stripping operation is given by $E_f=(q+1)eV_T$, where e is the charge on the electron and V_T the terminal voltage of the accelerator. In general, higher charge states correlate to higher achievable energies for a given acceleration device.

For gaseous or solid stripping media, the charge-state distribution of a particular ion beam reaches equilibrium after traversal of a certain thickness of the target material which is independent of the initial charge state of the incident ion beam. Solid-media strippers yield higher equilibrium charge states than their gaseous media counterparts. For example, the most probable charge state for a 20-MeV Pb^- ion beam passing through an equilibrium thickness of nitrogen gas (3.4×10^{15} atoms/cm^2) is 5, while that for a carbon foil (2.5×10^{17} atoms/cm^2) is 15 [1]. This difference in most probable charge state would correlate to a difference in final energy of 200 MeV for strippers placed in the terminal of a 20-MV tandem electrostatic accelerator. Thus higher charge states result in higher final energies. Differences in charge-state distributions between gaseous and foil strippers are attributable to the so-called density effect [2]; the key to the observed differences lies in the fact that electrons in high-lying, weakly bound levels, excited or captured in previous collisions, can be readily removed from the projectile in subsequent collisions, provided that the time between collisions is less than the radiative decay time ($\sim10^{-15}$–10^{-8} s) of these electronic states. [For example, the time between collisions for a 20-MeV projectile of mass 200 is 1.7×10^{-18} s in a solid stripper, compared to 1.1×10^{-8} s in a dilute gas stripper (1×10^{13} molecules/cm^3).]

In practice, carbon-foil lifetimes are limited by radiation damage, forward sputtering, and thermal and mechanical stresses which lead ultimately to foil breakage due to their fragility. The lifetime of a thin carbon foil of thickness t is affected by the energy E_1, the mass M_1, and atomic number Z_1 of the projectile and beam current density J striking the foil [3]. For example, for a Pb^- beam injected into a tandem accelerator operating at 20-MV terminal voltage, the injected beam intensity must typically be limited to $\sim$150 p nA to obtain a practical foil lifetime of $\sim$30 min. This beam intensity value is a factor of 20 to 30 lower than the 3–5 p μA which could otherwise be injected if foil lifetime was not a limiting factor.

Foil strippers also degrade the quality of heavy ion beams through multiple-scattering processes. For example, the half angle for multiple scattering as computed by use of the Sigmund-Winterbon theory [4] for a 5 μg/cm^2 carbon foil is $\sim$10 times greater than for a nitrogen target of 3.4×10^{15} molecules/cm^2 (thickness). On the other hand, the beam quality from gaseous strippers, while yielding lower charge states, is quite good. The limitations of these two commonly used strippers were the principal motivation for searching for an alternative stripping medium. A plasma, in principle, offers an attractive possibility as an alternative to either foil or gas stripping. In this report, we provide direct evidence that a low-atomic-number, highly ionized plasma, high-density target is much more effective in removing electrons from a high-energy heavy projectile than a neutral gas target of the same density.

II. PHYSICS BASES FOR A PLASMA STRIPPER

Stopping powers dE/dX (energy loss per unit length) for nonrelativistic projectiles passing through a plasma are different from those experienced by identical projectiles passing through a neutral gaseous target of the same line density [5]. In the projectile energy regime which is applicable for heavy ion stripping, electronic collisional processes are dominant. For a heavy ion of velocity V_1 interacting with completely ionized, neutral, or composite media, the stopping power appropriate for the respective medium can be expressed in terms of the approximate form of the Bethe, Bohr, and Bloch theory (see, for example, Ref. [6]):

Completely ionized plasma:

$$-dE/dx = \frac{4\pi Z_{1\,\mathrm{eff}}^2 e^4 n}{m_e V_1^2} Z_2 \ln\Lambda_{\mathrm{plasma}} ,$$

$$\Lambda_{\mathrm{plasma}} = \frac{1.123 m_e V_1^3}{\omega_p Z_{1\,\mathrm{eff}} e^2} , \quad (1)$$

neutral target:

$$-dE/dx = \frac{4\pi Z_{1\,\mathrm{eff}}^2 e^4 n}{m_e V_1^2} Z_2 \ln\Lambda_{\mathrm{neutral}} ,$$

$$\Lambda_{\mathrm{neutral}} = \frac{2 m_e V_1^3}{\bar{I}} , \quad (2)$$

partially ionized plasma target:

$$-dE/dx = \frac{4\pi Z_{1\,\mathrm{eff}}^2 e^4 n Z_2}{m_e V_1^2} (f_{\mathrm{neutral}} \ln\Lambda_{\mathrm{neutral}} + f_{\mathrm{plasma}} \ln\Lambda_{\mathrm{plasma}}) . \quad (3)$$

In expressions (1)–(3), $Z_{1\,\mathrm{eff}}$ is the effective charge of the ion during traversal of the respective medium of atomic number Z_2, e the charge on the electron, m_e the mass of the electron, n the number density of the target, $\bar{I}$ is the average excitation energy of the neutral target and ω_p the plasma frequency of the ionized target. In Eq. (3), f_{neutral} and f_{plasma} represent, respectively, the fraction of the target which is either neutral or ionized. Thus the stopping powers for heavy ions passing through a plasma are higher than those in a neutral target of the same density (1) due to the higher projectile charge state $Z_{1\,\mathrm{eff}}$ within a plasma, and (2) due to the greater magnitude of the argument of the Coulomb logarithm of the plasma $\Lambda_{\mathrm{plasma}}$ in comparison to that for a neutral target $\Lambda_{\mathrm{neutral}}$ at the same density n.

Experimental studies of the properties of hydrogen plasmas for possible inertial-confinement fusion applications have recently been conducted by Hoffmann and coworkers [7,8]. These authors have made comparisons of experimentally determined energy losses for 1.4-MeV/amu $^{40}Ca^{13+}$, $^{74}Ge^{18+}$, $^{84}Kr^{18+}$, $^{110}Pd^{26+}$, $^{208}Pb^{30+}$, and $^{238}U^{33+}$ projectiles interacting with fully ionized and neutral hydrogen targets as a function of line density. The measured stopping power of a particular plasma target was observed to be greater than that for the corresponding neutral target by factors ranging from 2 for ^{40}Ca to 2.6 for ^{238}U. The experimental values were found to agree closely with those predicted from expressions similar to those given by Eqs. (1) and (2) for the particular projectile hydrogen plasma and neutral hydrogen target combination. Two-thirds of the increase in dE/dx is attributed to the magnitude of the Coulomb logarithm for a plasma, while one-third of the increase is attributed to higher effective projectile charge states $Z_{1\,\mathrm{eff}}$ within the plasma medium in comparison to those within the neutral hydrogen target. Higher effective charge states within a particular medium are synonymous with higher charge-state distributions. These authors have also measured the charge-state distribution for a 4.8-MeV/amu $^{40}Ar^{10+}$ ion beam after passage through a fully ionized hydrogen plasma and found a most probable charge state of 16+ [8]; this result can be compared to an estimated value of 13+ for a neutral H_2 target and 16+ for a carbon foil target. Thus both theory and experiment support our original thesis that a highly ionized plasma composed of a properly chosen, low-atomic-number species, should be a more effective stripper than a neutral target of comparable thickness.

Still other qualitative physics arguments can be made which suggest that the charge-state distribution of a beam passing through a plasma should be higher than that for a neutral stripper. Higher charge-state distributions are expected when a low-atomic-number stripper is highly ionized due to the following effects.

(1) The number of available channels for projectile electron capture would be reduced by choice of a low-atomic-number, highly ionized target for projectiles in the 100–500-keV/amu energy regime.

(2) Projectile ionization could also take place by electron transfer from the projectile to the ionized target atom. (This channel is not available during interactions with a neutral target atom or molecule.)

(3) Projectile stripping would be enhanced and electronic capture would be inhibited by reduced screening of the low-atomic-number target nuclear charge.

(4) "Hot" electron cyclotron resonance (ECR) plasma electrons would be available for ionization of long-lived excited states of the projectile produced during previous projectile-target interactions.

(5) Angular scattering in the laboratory system will be only slightly higher than that of a neutral gaseous stripper and will be greatly reduced relative to a foil stripper.

III. COMPUTATIONAL SIMULATION APPROACH

A detailed and accurate description of the electron-loss and -capture processes which take place during interactions between a multielectron projectile and a multielectron target in various states of ionization presents formidable challenges to the computational theorist due to the many-body nature of the problem. Cross sections for the dominant electron-capture and -loss processes that take place during interactions between an energetic projectile A and a stationary target B must be extracted from representative interactions of the form

$$A^{q+}+B^{q'+}\rightarrow A^{(q-i)+}+B^{(q'-j)+}+(i+j)e\ ,$$
$$A^{q+}+B^{q'+}\rightarrow A^{(q+i)}+B^{(q'-j)}+(j-i)e \quad \text{for } j\geq i\ , \tag{4}$$
$$A^{q+}+B^{q'+}\rightarrow A^{(q-i)}+B^{(q'+j)}+(i-j)e \quad \text{for } i\geq j\ .$$

Theoretical solutions to many-body problems of this type and complexity necessarily require approximations which do not seriously compromise the basic physics which takes place during such interactions. Several theoretical options are available for consideration; the attributes and limitations of several of these approaches, along with the classical trajectory Monte Carlo method utilized in the present study, are described in Refs. [9–11]. The n-body classical trajectory Monte Carlo method (n-CTMC) was developed to circumvent many of the theoretical difficulties which confront other treatments of such problems. A very brief description of the methodology of the technique is given below. For more comprehensive details of the n-CTMC technique, the reader is directed to the references cited above.

The n-CTMC model directly includes all interactions between the respective nuclei and all active electrons associated with either the projectile or the target in a two-center screened potential interaction representation. The method includes the equivalent of an infinite basis set which spans the discrete electronic states, as well as ionization continuum. Electron orbits, determined from the sequential binding energies of the electrons, are used for each of the electrons attached to each of the interacting partners. In order to represent projectile-plasma, projectile-neutral interactions with reasonable accuracy, cross sections for all important projectile electron-capture and -loss processes must be included. The n-CTMC method requires the numerical solution for several thousand trajectories of a multielectron projectile interacting with a multielectron target under the influence of a two-center screened potential covering a wide range of impact parameters. The Hamiltonian for reactions between a projectile of momentum p_A and mass M_A with a target of momentum p_B and mass M_B to each of which are attached electrons of momenta p_{iA}, p_{iB}, and mass m_e, respectively, as described by Eq. (4), can be written as

$$H=p_A^2/2M_A+p_B^2/2M_B+\sum_{i=1}^{N}p_{iA}^2/2m_e + \sum_{i=1}^{M}p_{iB}^2/2m_e+V_{A,B}(r) \tag{5}$$

where $V_{A,B}(r)=V_A(r_A)+V_B(r_B)$. In this approximation, the active electron is assumed to interact simultaneously with a target B and projectile A through the two-center potential given by

$$V_{A,B}(r)=\frac{1}{r}[N_{A,B}S_{A,B}(r)-Z_{A,B}] \tag{6}$$

with

$$S_{A,B}(r)=1-\{(\eta_{A,B}/\epsilon_{A,B})[\exp(\epsilon_{A,B}r)-1]+1\}^{-1}$$

where $Z_{A,B}$ and $N_{A,B}$ are the nuclear charge and number of inactive electrons attached to the projectiles and target cores, respectively, and $\eta_{A,B}$ and $\epsilon_{A,B}$ are screening parameters of the respective interacting partners determined from Hartree-Fock calculations as described in Ref. [10]. Cross sections, for specific projectile-A–target-B interactions as represented by Eq. (4), are obtained by solving the equations of motion for thousands of trajectories using the n-CTMC method. The resulting cross sections are then introduced into a system of coupled rate equations as represented by the following expression:

$$\frac{d^2N_q}{dxdt}=n_{j,j-1}\frac{dN_{q-1}}{dt}\sigma_{q-1,q}+n_{j,j+1}\frac{dN_{q+1}}{dt}\sigma_{q+1,q} -n_{j,j-1}\frac{dN_q}{dt}\sigma_{q,q+1}-n_{j,j+1}\frac{dN_q}{dt}\sigma_{q,q-1} \tag{7}$$

which describes the evolution of the number of particles N_q in charge state q per unit time dt and distance dx within the target media. In Eq. (7), $n_{i,j}$ represents the number density of target ions/atoms which are in initial states of ionization i and final states j and $N_{q'}$ are the number of projectiles in initial state q' entering the interaction which proceeds with cross sections $\sigma_{q',q}$.

Collisions of the projectile with the electrons in the plasma were also evaluated. However, because of the inherent low temperature of the plasma ($\langle T\rangle\approx 10$ eV), the effective electron collision energy is determined by the translational velocity of the projectile, which leads to $E_e\approx 50$ eV. For collisions with ground-state Pb^{q+} ions, the electrons were ineffective above $q=3$ because the projectile binding energy exceeds the electron's translational energy. Contributions to stripping cross sections resulting from interactions between both electron and ion plasma constituents with excited states of the projectile formed in previous collisional excitation or electron-capture processes were also included. However, these processes only marginally increased the projectile charge states due to the low collisional frequency between the projectile and the plasma constituents, which allowed the excited-state populations to decrease to low values through radiative decay processes. On the other hand, electron-capture processes from the 20-MeV Pb projectile to the plasma nuclei were found to contribute significantly to the stripping cross sections. Such channels are not available when a neutral target is used as a stripper.

In order to evaluate the appropriateness of the n-CTMC model for performing the calculations required in the intended study, comparisons were made with experimental measurements. Figure 1 displays computed and experimentally measured charge-state fractions resulting from interactions between 12-MeV I projectiles and a H_2 target [12]. The calculated and measured charge-state distributions are seen to agree precisely in terms of the most probable charge state and agree within a factor of less than 2 in absolute magnitude for a particular charge state. Considering the potential difficulties associated with accurately measuring the charge-state distributions emerging from a H_2 target, the agreement is believed to

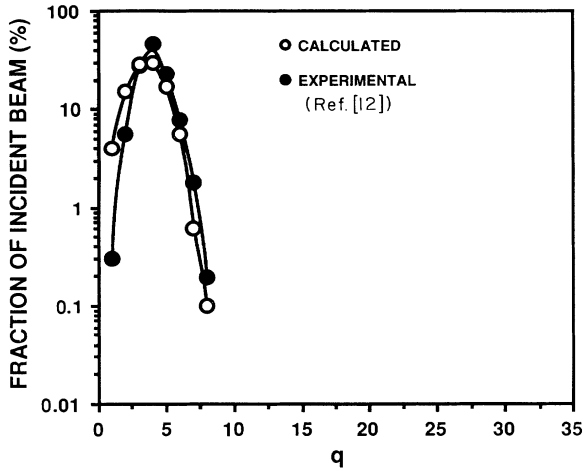

FIG. 1. Comparison of calculated and experimentally measured equilibrium charge-state fractions vs charge-state q projectiles for 12-MeV I interacting with a H_2 target.

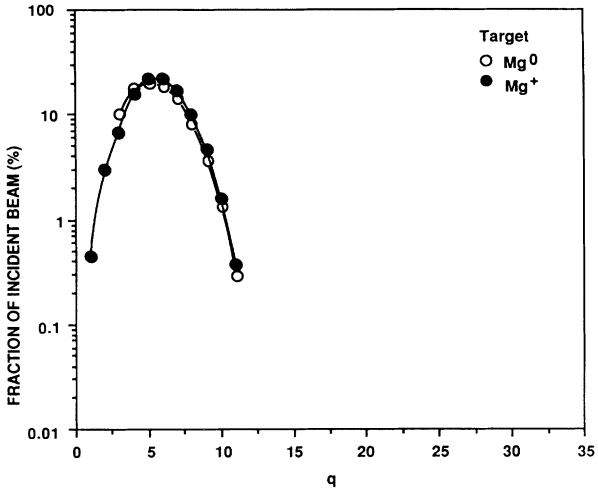

FIG. 2. Calculated equilibrium charge-state fractions vs charge state q for 20-MeV Pb projectiles interacting with neutral Mg^0 and fully ionized Mg^+ plasma targets.

be quite good, thus lending confidence in our choice of the n-CTMC model for use in the present studies.

IV. COMPUTATIONAL STUDIES

The ultimate objective of the study is to evaluate the feasibility of using a plasma to enhance heavy projectile equilibrium charge states over those achievable by conventional neutral gaseous strippers. In order to achieve this objective, a system must be found for which projectile stripping is enhanced and projectile electron capture is suppressed. A plasma can possess these characteristics, provided that a suitable target can be found where the capture and loss cross sections behave in the desired manner. Since electron capture is also likely to occur from the inner shells of the target, a plasma composed of highly ionized heavy atoms may not improve the projectile equilibrium charge states appreciably, whereas a light target with few electrons to capture should improve the charge-state distribution over that from a neutral target. In order to illustrate this point, we chose to study interactions between a 20-MeV projectile during passage through Mg and Mg^+, Li^0 and Li^+, and H_2^0 and H^+ targets. In all cases involving a plasma, the targets are assumed to be fully ionized.

The equilibrium values for the charge-state distribution versus line density for 20-MeV Pb ions incident on a particular ion or atom were calculated for each of the indicated strippers. The equilibrium charge-state distributions for Mg^0 and Mg^+ targets, as represented by the fractions of the Pb^{q+} beam in a particular charge state q, are shown in Fig. 2. as noted, only modest improvements in the charge-state distribution of Pb ions can be realized ($\sim 25\%$ for the high charge side of the distribution) if magnesium is chosen as our target material, due to the fact that electron capture from the $2s$ and $2p$ subshells occurs with high probability for the chosen projectile and projectile energy. Moreover, the theoretical studies indicate that the line density necessary to approach equilibrium is approximately 5×10^{15} ions/cm^2. It is obvious that a better candidate system must be chosen in order to maximize the plasma stripping effect.

As a result of exploratory calculations of interactions between 20-MeV Pb projectiles and Cs^+ and Na^+ plasma targets which yielded results similar to those obtained for Mg^+ plasma targets, we were led to try even lower Z_2 target elements. The number of electron-capture channels can be reduced significantly if we choose a lower-atomic-number stripper such as Li. The effect can readily be seen by comparing the equilibrium charge-state distribution for 20-MeV Pb projectiles interacting with Li^0 and Li^+ targets as shown in Fig. 3. (The charge states are compared at target thicknesses of $\sim 2\times 10^{16}$ cm^{-2}.) The most probable charge state for Li is ~ 4, while that for the Li^+ is ~ 6, which correlates to a final energy

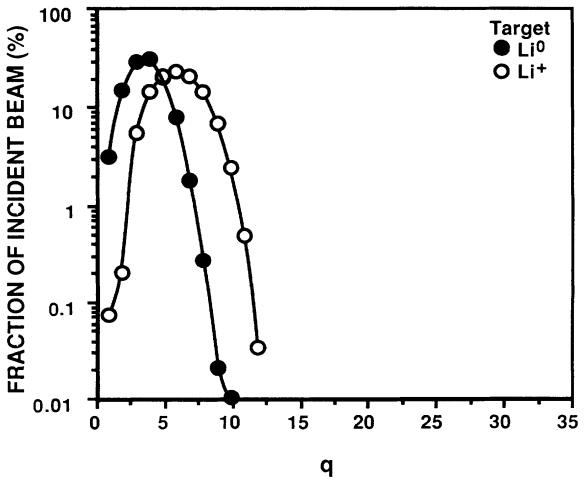

FIG. 3. Calculated equilibrium charge-state fractions vs charge state q for 20-MeV Pb projectiles interacting with neutral Li^0 and fully ionized Li^+ plasma targets.

difference of 40 MeV for a stripper mounted in the terminal of a 20-MV tandem accelerator. As noted, Li^+ improved the charge-state distribution considerably better than did Mg^+ due to the decreased cross sections for K-shell capture from Li^+ relative to that of M-shell capture from Mg^+. The limit of this selection process is, of course, hydrogen.

Similar calculations were performed for H_2^0 gaseous and H^+ plasma targets. The dependence of the various Pb projectile charge states versus H^+ line density are shown in Fig. 4. The fractions of the incident beam in a particular charge state q are shown in Fig. 5 for a neutral hydrogen target at equilibrium and for a fully ionized hydrogen target at several line densities. An equilibrium charge-state value of 3.4 was realized for the Pb ion incident on neutral hydrogen. This value is much lower than the 5.2 expected for higher Z_2 gas targets. The reason for this behavior for the neutral target is that the capture channel is as strong as in the higher Z_2 elements due to good overlap of the target's electron velocity distribution with that of the 20-MeV Pb ion. However, the competition from stripping of electrons from the Pb ion is reduced due to the low Z_2 of the hydrogen nucleus which inhibits increases in the stripping cross section during collisions with the plasma nucleus. Because of this effect, the line density needed to reach an equilibrium charge-state distribution for the neutral hydrogen target is approximately an order of magnitude larger than for the higher Z_2 Mg case shown in Fig. 2. Conversely, a hydrogen plasma possesses an important attribute required to strip Pb ions to high charges states—namely, the attribute that there are no significant electron-capture channels available which result in reducing the Pb charge as the ion transverses the plasma target. (Radiative recombination cross sections have a negligible effect at the densities investigated.) Thus, the only inelastic scattering channels available are stripping by the plasma electrons and protons. As shown in Fig. 5, our calculations indicate that charge-state distributions competitive with foils are realized at line densities of $\sim 10^{18}$ ions/cm^2. Hydrogen plasma line densities of greater than 10^{19}/cm^2 have already been obtained by Hoffmann and co-workers [7,8]. At a plasma line density of 10^{19} ions/cm^2, we estimate

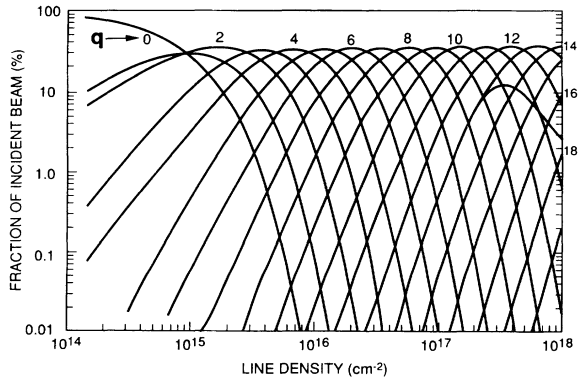

FIG. 4. Calculated dependence of various charge states q on line density for 20-MeV Pb projectiles interacting with a fully ionized H^+ plasma target.

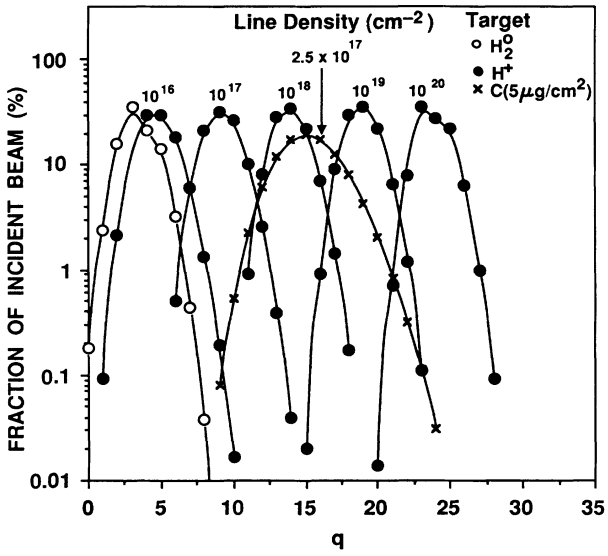

FIG. 5. Calculated variation of charge fraction vs charge state q for 20-MeV Pb projectiles interacting with fully ionized hydrogen targets at several line densities. Also shown are the charge-state distributions at equilibrium for neutral hydrogen and thin carbon-foil targets.

that a most probable charge state for the Pb ion of ~ 19 would be obtained (Fig. 5). Furthermore, equilibrium charge-state distributions are not realized with the hydrogen plasma. This effect is illustrated in Fig. 5 and reinforced in Fig. 6, which displays most probable charge state $\langle q \rangle$ for the Pb projectile as a function of target line density. Also shown for comparison, in Fig. 5, are the most probable charge states which occur for equilibrium target thicknesses for neutral hydrogen and a thin (5-μg/cm^2) carbon foil. From these results, we note the importance of increasing the plasma line density for producing higher charge states of the Pb projectile.

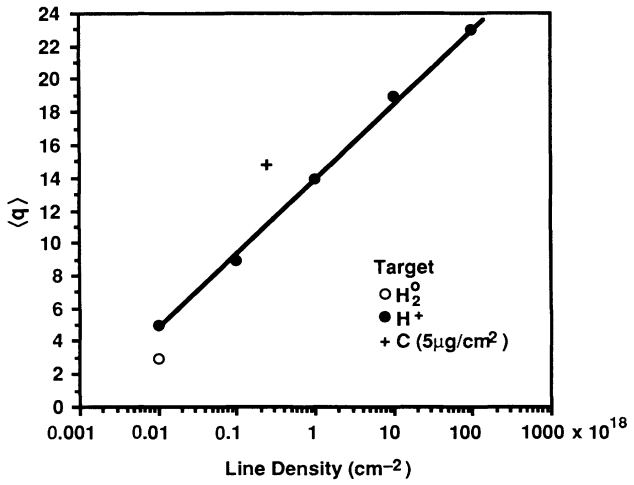

FIG. 6. Calculated variation of most probable charge state $\langle q \rangle$ with line density for 20-MeV Pb projectiles interacting with a fully ionized hydrogen target. Also shown are similar results for equilibrium target thickness of neutral hydrogen and a thin carbon-foil stripper.

V. MULTIPLE-SCATTERING EFFECTS

Multiple scattering can seriously and deleteriously affect beam quality and, consequently, beam transmission following the stripping process when foil strippers are used, particularly for heavy projectiles with energies in the range of a few to several tens of MeV. The beam component which is lost can result in loading of the high-voltage terminal power supply and can induce serious sparking in the high-voltage electrode structure. A plasma stripper is expected to approximately emulate the scattering properties of a gas stripper of the same atomic number Z_2. However, because of the increase in stopping power of the plasma in relation to that of the neutral stripper, the energy straggling within the beam will be greater for a plasma than for a neutral stripper [see, e.g., Eq. (1)]. The n-CTMC model can be used to estimate multiple scattering by accumulating the scattering information of the projectile during passage through a particular target. Figure 7 displays the multiple scattering half angle α versus the fraction F of the beam included within the half angle as a function of H^+ line density. Results from Sigmund-Winterbon calculations for N_2 ($3.4\times10^{15}/cm^2$) and C-foil ($2.5\times10^{17}/cm^2$) strippers are also shown for comparison. As noted, multiple scattering from the carbon-foil stripper is $\sim$15–45 times greater than from a H^+ plasma at equivalent line densities, while a N_2 stripper degrades the beam quality by a factor of 10–30 over that of a H^+ stripper, again, at equivalent line densities.

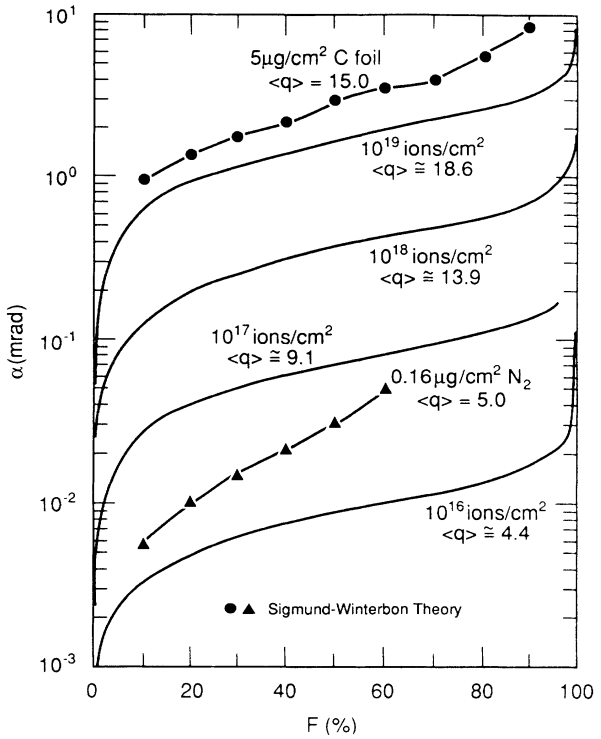

FIG. 7. Scattering angle α fraction for 20-MeV Pb projectiles interacting with a fully ionized H^+ plasma at various line densities. The most probable charge states $\langle q \rangle$, resulting from the projectile-target interactions, are also shown.

VI. DISCUSSION

From these studies, we have clearly demonstrated for the first time that a highly ionized, low-atomic-number stripper can be much more effective in removing electrons from energetic projectiles than can a neutral stripper of the same density. These results thus support our initial intuitive belief that a plasma might have beneficial stripping attributes. We also show that the n-CTMC model is a powerful tool for describing the complex physical processes involved during projectile-target interactions which would be difficult to simulate with other theoretical models. For example, the model can be used to realistically predict charge-state distributions resulting from passage of high-energy, heavy, multielectron projectiles through neutral gaseous or plasma targets in various states of ionization.

As evidenced from this study, the differences in charge states for 20-MeV Pb projectiles which result when Mg^+, Li^+, or H^+ plasma targets are chosen are quite dramatic. A fully ionized H^+ plasma is obviously the best choice for a stripper because there are essentially no channels available for electron capture by the projectile and the angular scattering of the projectile in the laboratory system is considerably reduced over that resulting from the use of a high Z_2 target. As a consequence, a hydrogen plasma stripper does not reach a limiting equilibrium charge-state distribution for plasma line densities up to $10^{20}/cm^2$ as is found for neutral and single-charged higher Z_2 plasma strippers. Higher charge states can be achieved by simply increasing the line density as shown in Fig. 6. However, in order to produce a practical stripper which is competitive with a foil stripper, a hydrogen plasma line density of $\sim10^{18}/cm^2$ must be achieved (Fig. 6). Hoffmann and co-workers [7,8] have been able to generate plasma line densities in pulsed mode of $\geq 10^{19}/cm^2$. However, the high degree of ionization, the line density, and consequential power requirements for producing charge states competitive with those from a C-foil stripper with a plasma stripper operated in a cw mode, poses serious challenges, for example, to the state-of-the-art ECR technology where densities of only $10^{14}/cm^3$ have recently been achieved [13].

ACKNOWLEDGMENT

Research for this paper was sponsored by the U.S. Department of Energy under Contract No. DE-AC05-84OR21400 with Martin Marietta Energy Systems, Inc.

[1] Computed with the program described by R. O. Sayer, Rev. Phys. Appl. **12**, 1543 (1977).
[2] N. Bohr and J. Lindhard, K. Dan. Vidensk. Selsk. Mat.-Fys. Medd. **28**, (1954).
[3] R. L. Auble and D. M. Galbraith, Nucl. Instrum. Methods **200**, 13 (1982).
[4] P. Sigmund and K. B. Winterbon, Nucl. Instrum. Methods **119**, 541 (1974).
[5] C. M. Jones, G. D. Alton, J. B. Ball, J. B. Biggerstaff, D. T. Dowling, K. A. Erb, D. L. Haynes, D. E. Hoglund, E. D. Hudson, R. C. Juras, S. N. Lane, C. A. Ludemann, J. A. Martin, S. W. Mosko, D. K. Olsen, E. G. Richardson, P. H. Stelson, and N. F. Ziegler, Nucl. Instrum. Methods A **244**, 7 (1985).
[6] J. D. Jackson, *Classical Electrodynamics* (Wiley, New York, 1975), Chap. 13.
[7] D. H. H. Hoffmann, K. Weyrich, H. Wahl, D. Gardnes, R. Bimbot, and C. Fleurier, Phys. Rev. A **42**, 2313 (1990).
[8] D. H. H. Hoffmann, K. G. Dietrich, W. Laux, E. Boggasch, K. Mahrt-Olt, H. Wahl, A. A. Golubev, and V. P. Dubenkov, Z. Phys. D **21**, S105 (1991).
[9] R. E. Olson, J. Ullrich, and H. Schmidt-Böcking, Phys. Rev. A **39**, 5572 (1989).
[10] C. O. Reinhold, D. R. Schultz, R. E. Olson, L. H. Toburen, and R. D. Dubois, J. Phys. B **23**, L297 (1990).
[11] D. R. Schultz, R. E. Olson, C. O. Reinhold, S. Kelbch, C. Kelbch, H. Schmidt-Böcking, and I. Ullrich, J. Phys. B **23**, 3839 (1990).
[12] A. B. Wittkower and G. Ryding, Phys. Rev. A **4**, 226 (1971).
[13] P. Zhu and R. W. Boswell, Phys. Rev. Lett. **63**, 2805 (1989).